Numerical Calculation of Roll Pass Designs for 3-Roll Rolling Mills

Author

Christian Overhagen, Assistant Professor, University of Duisburg-Essen, Chair of Metallurgy and Metal Forming, Duisburg, Germany
christian.overhagen@uni-due.de

After a mechanical rolling model for the 3-roll process was already presented by the author in 2013, the present work focuses on a numerical algorithm for roll pass design in 3-roll rolling mills. The algorithm is based on geometric parametrizations of the used groove geometries, as well as an equivalent flat-pass method in conjunction with a spreading model. The novel method allows the calculation of the groove geometries of a pass sequence to achieve a target cross-sectional distribution without over- or underfilling of the individual grooves. The algorithm uses a nonlinear numerical optimization technique to determine the geometric data of the groove geometries. Examples are shown for typical rolling tasks on continuous mills in the 3-roll method. The model provides a framework for further developments, as it allows the integration of more sophisticated spreading models. The source codes in MATLAB will be made publicly available.

Introduction

In the production of steel wire rod and bars, the longitudinal rolling process has proven to be the most reliable and economical production route. A problem is to control section deviations along the length of a rolled material strand, as shown in Reference 1. Therefore, rolling processes that are insensitive to variations of the inlet material are sought out. A tremendous source of section deviations is the free lateral spread encountered during hot rolling and influenced by material temperature and composition as well as interstand tensions.[2] Nowadays, the 3-roll rolling process is known to show only a limited amount of free spreading compared to the classical 2-roll rolling process. However, the roll pass design of such 3-roll mills is not easy to accomplish since there is no alternating sequence of minor grooves and major grooves which can be designed separately as in the 2-roll process. In the beginning of the process, only the entry and exit section is known. Precise simulations can be carried out using the finite element method (FEM), but the computational effort required for such simulations is much too high for, say, a pass design office at a mill building company, where a high number of pass designs must be determined each day.

Therefore, the roll pass design problem seeks for a fast numerical solution algorithm. Based on the rolling model for the 3-roll process which was presented 10 years ago,[3] this article shows a computational method for the determination of roll pass designs for the 3-roll process based on nonlinear optimization technique using the equations describing the groove geometries and spread calculation. The model is first applied to a single pass to show the principal dependencies of the groove geometries. Finally, the methodology is applied to a complete pass design for a 6-stand rolling block in the 3-roll rolling method.

Recently with the PyRolL project,[4] an open-source framework for rolling simulation of long products became available. The MATLAB source code used in the current article is maintained at a GitHub

repository, available to the public for further development (see Conclusions section).

Hot Rolling of Circular Sections in 3-Roll Mills

The 3-roll rolling technology has become widely accepted to produce wire rod and bars in close tolerances. Generally, a rolling process where several N rolls are directly used to form the deformation region, the rolls are arranged in an angle of 360°/N. That is, the roll axes are arranged at an angle of 180° (parallel) to each other in the 2-roll process (2RP), but at an angle of 120° to each other in the 3-roll process (3RP), as shown in Fig. 1.

Typically, a 3-roll mill is used within a bar mill as a finishing mill, or also to size key cross-section, for instance before final rolling in a high-speed finishing block. Typical advantages of the 3RP over the 2RP are a higher definition of the rolled cross-section as a higher fraction of the section circumference is bound to roll surfaces. Also, the distribution of the total deformation on three rolls instead of two rolls leads to lower height reductions per roll and therefore lower force, work, and power consumptions. The different deformation distribution in the process also leads to changes in the spreading behavior during hot rolling. The phenomenon of spreading in the rolling process is directly connected to the existing complexity of the pass design. An exact prediction of the lateral spread is crucial for working out pass design for hot rolling of long products. As was shown earlier,[6] the 3-roll process also shows less significant sensitivities for different spreading behavior of a wide range of materials.

However, a fast and precise method of automated roll pass design is still missing in the literature. This article aims to provide a means to fill this gap with the presentation of an extensible computational model.

Spread Calculation for 3-Roll Rolling Mills

A review on methods for spread calculation in the 2-roll rolling model was given by Mauk and Kopp in 1983.[7] Using the empirical methods described in their paper, it is possible to calculate the spread in 2-roll hot flat rolling with high precision. Mauk found that a set of general spread equations can be described by the following approach:

$$\left|\frac{\varepsilon_w}{\varepsilon_h}\right| = C_1\left(\frac{w_0}{h_0}\right)^{C_2} e^{C_3\left(\frac{w_0}{h_0}\right)^{C_4}\left(\frac{w_0}{l_d}\right)^{C_5}\left(\frac{w_0}{R}\right)^{C_6}\left(\frac{w_0}{R}\right)^{C_7}\left(\frac{\Delta h}{h_0}\right)^{C_8}}$$

(Eq. 1)

where

ε_w and ε_h = the global true strains in width and height direction,

w_0 = the initial width,

h_0 and h_1 = the initial and final heights,

R = the roll radius and

l_d = the contact length given as $l_d = \sqrt{R\left(h_0 - h_1\right)}$.

If sufficient practical results are available, this approach can also be used to create a spreading model for the hot rolling of flat passes in 3-roll mills.

Currently, a sufficiently large set of such rolling trial data is not freely available for the 3RP. Therefore, the

Figure 1

Roll arrangement in the 3-roll rolling process and the formation of a groove between the roll surfaces.[5]

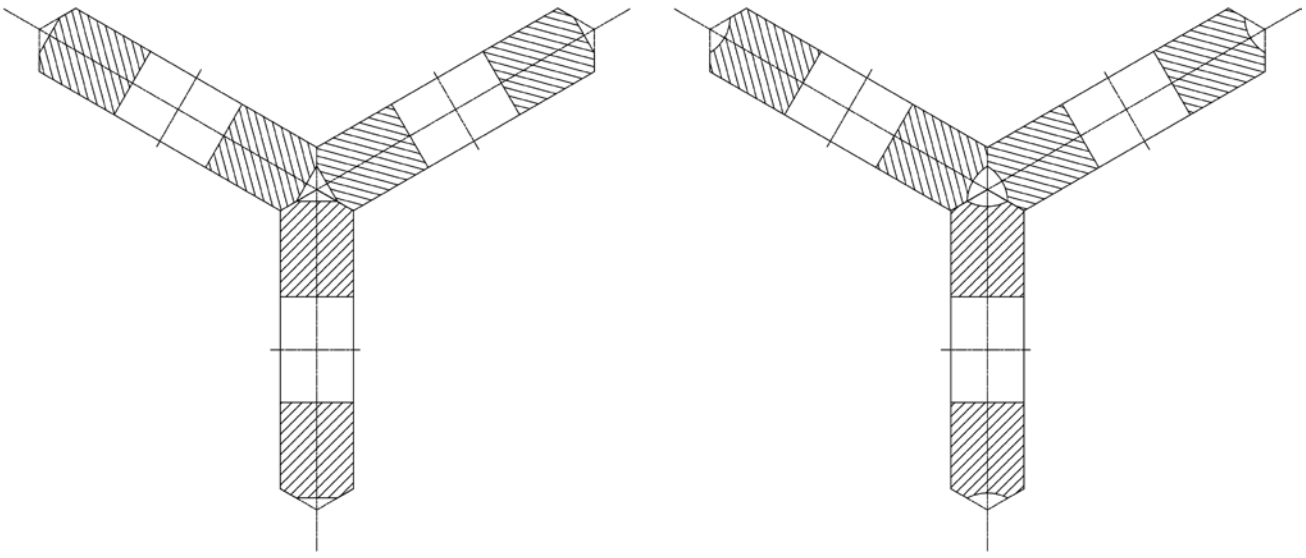

deformation characteristics of the 2RP and 3RP must be examined with respect to one another to provide a calculation basis for the spread in the 3RP which is based on the known models for the 2RP.

Apart from Eq. 1, another spread equation for 2RP which has proven itself was given by Marini based on theoretical considerations:[8]

$$b_1 = b_0 + \frac{\Delta h b_0 \left(R - \frac{h_0}{2}\right) B}{h_1 b_0 + \frac{b_0 (h_0 + h_1)}{2} \cdot \frac{1+A}{1-A} \cdot \frac{0.91(b_0 + 3h_0)}{4h_0} + 2h_1 RB};$$

$$A = \frac{\sqrt{\Delta h}}{2\mu\sqrt{R}}; B = \sqrt{\frac{\Delta h}{R}}$$

(Eq. 2)

Another advantage of Marini's equation is that it considers the physical friction coefficient μ.

Fig. 2 shows the deformation regions of the 2RP and 3RP rolling processes for the basic flat passes. In the 2RP, the characteristic flat-pass geometry is that of a rectangle; in the 3RP, it is that of a hexagon.

A major and very important difference is the definition of the heights and widths. As in the 2RP, it is possible to measure the width and height linearly in one direction. However, in the 3RP, the heights and widths must be defined in relation to the center of the groove, in directions against the roll surface and the free spreading surface, respectively. Therefore, the heights and widths are measured in a radial sense in the 3RP.

For an irregular hexagon like the exit section shown in Fig. 2a, the cross-sections of the entry and exit sections are calculated from:

$$A_{0,3} = 4b_{0,3}h_{0,3} - {h_{0,3}}^2 - {b_{0,3}}^2$$
$$A_{1,3} = 4b_{1,3}h_{1,3} - {h_{1,3}}^2 - {b_{1,3}}^2$$

(Eq. 3)

The shared core cross-section (non-shaded area in Fig. 2a) is given as:

$$A_{c,3} = 4b_{0,3}h_{1,3} - {h_{1,3}}^2 - {b_{1,3}}^2$$

(Eq. 4)

The elongation efficiency of the 3RP for a flat pass is then:

$$f_{s,3} = 1 - \frac{A_{1,3} - A_{c,3}}{A_{0,3} - A_{c,3}}$$
$$f_{s,3} = 1 - \frac{\Delta b_3 \left(b_{0,3} + b_{1,3} - 4h_{1,3}\right)}{\Delta h_3 \left(h_0 - 4b_0 + h_{1,3}\right)}$$

(Eq. 5)

In the 2RP, a general spreading equation would be a function of the following type, relating the width increase to the height reduction, for a set of given rolling conditions represented by the vector C (including other geometrical parameters, friction, temperature and material):

Figure 2

Spreading characteristics of the 3RP (a) and the 2RP (b).

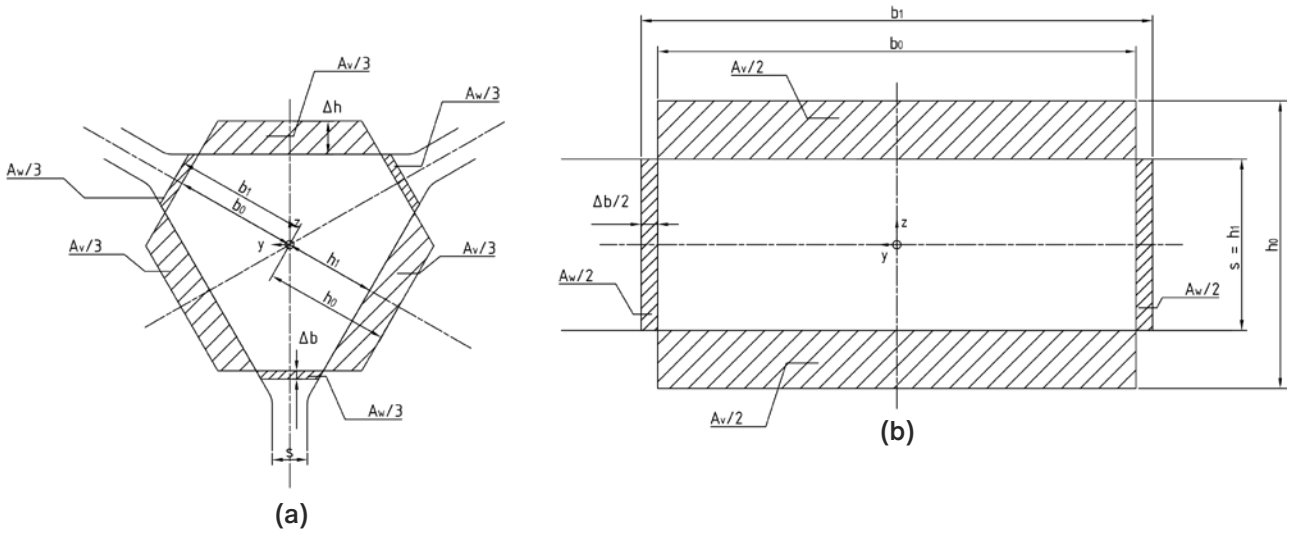

$$\Delta b = b_1 - b_0 = f\left(\Delta h\right)_C$$

(Eq. 6)

Attributing the width change on each of the two sides of the rolled bar to the height reduction contribution of each roll and transferring this to the 3RP, one can write:

$$\Delta b_3 = \frac{1}{2} \cdot f\left(2\Delta h_3\right)_C$$

(Eq. 7)

This simple transformation between the spreading relations allows an approximate of the spreading in the 3-roll process to be calculated. More precise spreading calculations might be achieved by the application of the upper bound theorem as outlined in Reference 9. Analytical equations for the spread in the 3RP based on finite element method simulations were given by Min et al.[10] for discrete classes of pass geometries. However, the current analysis will stick to the transfer model as given earlier in combination with Marini's spread equation, but it should be emphasized that any other spread model can also be included in the software framework presented here.

For the spread calculation considering non-flat sections, a hexagonal equivalent pass method must be employed. A logical transfer of Lendl's rectangular pass method to the 3RP was given in Reference 3.

Fundamentals of Roll Pass Design for 3-Roll Rolling Mills

The procedure of roll pass design contains all necessary steps to determine the geometry of all roll grooves which are necessary to produce a predefined final section out of a suitable starting section. Nowadays, the definition of geometrical groove shapes must adhere to technological, economic and ecological criteria. Usually, the number of passes should be as low as possible to minimize energy consumption and cost.

A 3-roll mill, as embedded in a bar or wire rod mill, will take a round section coming from a 2-roll rolling process as the initial section and transform it into a smaller round section with tight tolerances. Generally, the total reduction of a pass sequence in a 3-roll rolling block might be expressed as:

$$\lambda_{total} = \lambda_1 \cdot \lambda_2 \cdot \ldots \cdot \lambda_N = \lambda_m{}^N$$

(Eq. 8)

Here, λ_m is a mean per-pass reduction to represent the reduction potential of the rolling process to be applied. The fundamentals of pass design are also given in Reference 11.

In a 3-roll rolling mill, a few characteristic groove shapes can be found. These can be (but are not limited to):

- Flat grooves, where all three rolls have flat groove barrels.
- Single-radius round grooves (non-opened).
- Opened single-radius round grooves.
- Double-radius round grooves.

Each of these groove geometries can now be parametrized by means of a restricted set of numerical parameters, as it can be seen from Fig. 3. The flat groove is uniquely defined by its inner radius IR, as well as the roll gap s and the transition radius R2 (roll barrel to roll gap). Therefore, when these three parameters are known, the groove geometry can always be precisely reproduced.

The flat groove (see Fig. 3a) is uniquely determined by the inner radius (IR), the roll gap s and the radius R2, which indicates the transition radius from the roll barrel to the roll gap.

The general non-opened single-radius round (see Fig. 3b) additionally has a rounded barrel shape with a finite main radius R1. Still, the inner radius IR is used to characterize the size of the groove. The groove can eccentric, as shown in Fig. 3b when R1 > IR. The eccentricity of the groove is characterized by the relation e = R1/IR.

Therefore, for the unique definition of this groove, the data of the inner radius IR, the main groove radius R1 as well as the roll gap data s and R2 are required.

Practically, the single-radius grooves might be used in a variant where they are tangentially opened. This is shown in Figs. 3c and 3d.

The result is a groove that is less sensitive to spreading variations as it introduces an additional spreading safety. For a unique definition of this groove type, the following data are required: IR, R1, alpha, R2 and s.

Table 1 gives an overview of the groove data that are required to uniquely define each of the groove types.

To enable the numerical evaluation of the filling conditions of each of these groove types numerically, it is important to be able to calculate the width on face (wof) of the grooves. Under no circumstances should the grooves be filled with a section width greater than the wof.

For the simple flat groove according to Fig. 3a, the width on face is:

Figure 3

Groove geometries for 3-roll rolling blocks: Flat roll barrel (a), single-radius groove (eccentric) (b), opened single-radius groove (non-eccentric) (c) and opened single-radius groove (non-eccentric) (d), from Reference 5.

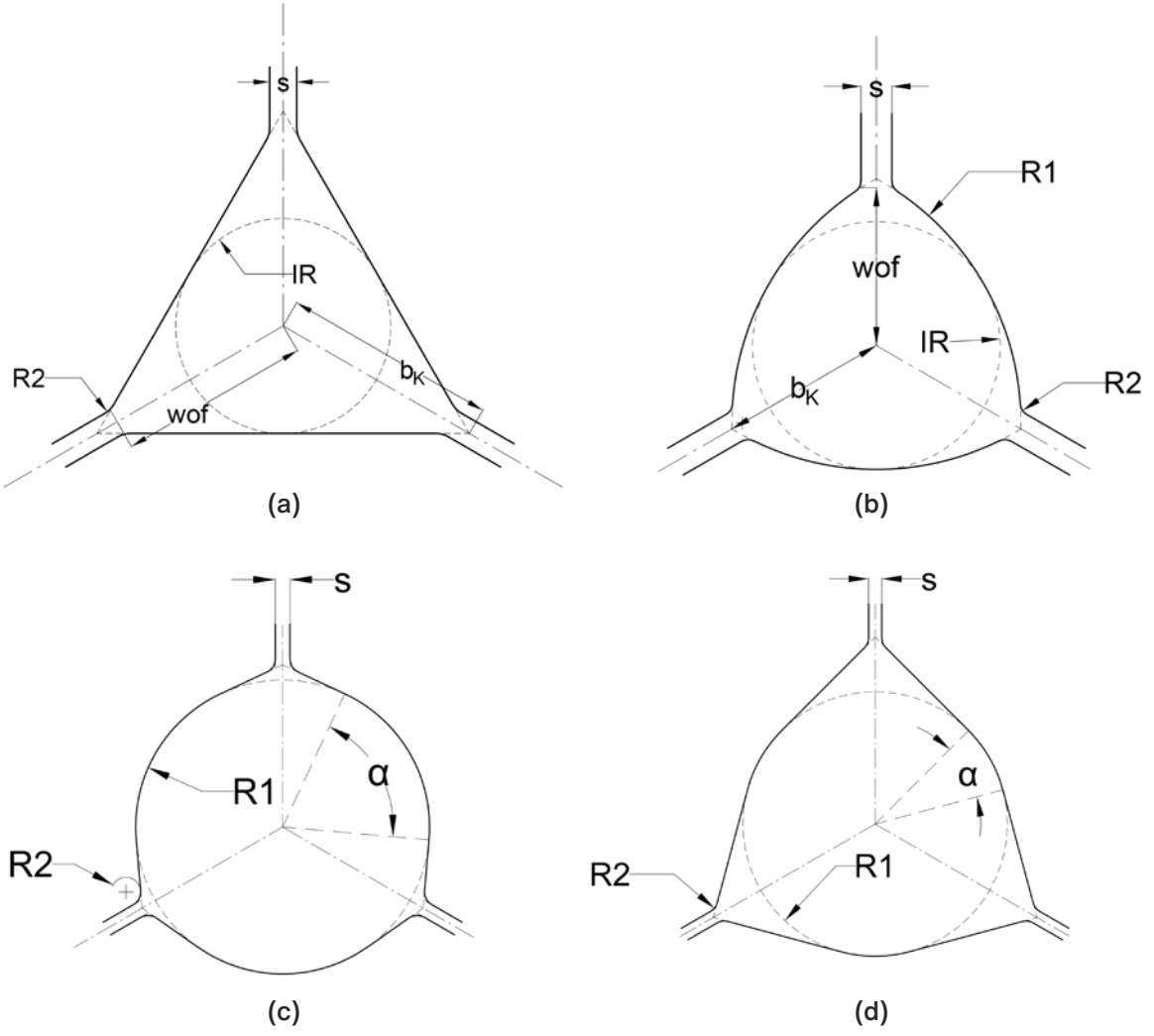

$$wof = 2IR - \frac{\sqrt{3}}{2}s$$

(Eq. 9)

For the non-opened single-radius groove, one has to additionally account for the main radius R1 of the groove and arrive at:

$$wof = \sqrt{R_1^2 - \left(\frac{\sqrt{3}}{2}(R_1 - IR) + \frac{s}{2}\right)^2} + \frac{1}{2}(IR - R_1)$$

(Eq. 10)

For the opened single-radius groove, refer to Fig. 4, where some additional geometric values

Table 1

Geometrical Parameters Necessary for the Definition of the Groove Types Shown in Fig. 3

	RI inner radius	R1 primary radius	R2 trans. radius	Alpha groove angle	s roll gap
Flat groove	X		X		X
Single radius	X	X	X		X
Single-radius opened	X	X	X	X	X

Figure 4

About the determination of the width on face of the opened single-radius groove.[5]

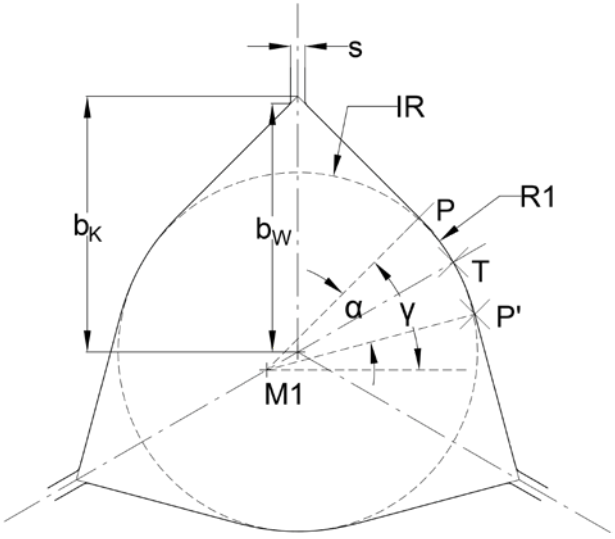

are defined (b_W = wof). The points P and P' are the tangent points where the main radius and the tangential opening lines intersect. The point T is the intersection of the main radius with the 60° symmetry line of the groove. M1 is the center point of the main radius R1. The angle γ is additionally defined as γ = 30° + α/2.

Finally, the wof of the opened groove can be expressed according to:

$$wof = \frac{1}{2}\left(IR - R_1\right) + R_1 \sin\gamma - \tan\left(90° - \gamma\right) \cdot \left(\frac{\sqrt{3}}{2}\left(IR - R_1\right) + R_1 \cos\gamma - \frac{s}{2}\right)$$

(Eq. 11)

The groove filling will then be evaluated numerically by means of the filling ratio f_f given as the actual section width related to the wof of the groove:

$$f_f = \frac{b_1}{wof}$$

(Eq. 12)

A Software Algorithm for Roll Pass Design of 3-Roll Grooves

Using the definitions and the spread calculation presented earlier, one can find the groove geometry of a given class to produce a prescribed exit cross-section A1 at a given initial section and a target filling ratio of the groove.

Basically, by variation of the groove parameters given in Table 1, one can optimize the groove geometry fulfill these criteria.

The construction of the parametrized groove geometries is expressed as functions that take the geometry parameters as input value and return the numerical contour of the constructed groove. In the MATLAB code, these are the functions:

groove_threeroll_flat(ir, r2, s)
groove_threeroll_singleradius(ir, r1, r2, s)
groove_threeroll_singleradius_opened(ir, r1, r2, alpha, s)

The output MATLAB structure contour includes these and more calculated geometrical parameters of the groove, and most importantly, the x- and y-coordinates of the final contour in contour.xy for the complete contour and also separately for each one of the three rolls in contour.roll1xy, contour.roll2xy and contour.roll3xy.

The functions design_flat, design_singleradius and design_singleradius_opened carry out a pass calculation on one of these groove types with prescribed groove data, yielding the filling ratio, as well as the cross-section of the exit section. These values are then compared to the user-supplied target values, and a residual is calculated according to:

$$res = \sqrt{\left(A_1 - A_{1,tgt}\right)^2 + \left(f_f - f_{f,tgt}\right)^2}$$

(Eq. 13)

The input vector x to these functions contains the assumed input values inner radius ir of the groove and the eccentricity relation ecc = r1/ir.

The design_xxx functions would calculate the residual for given groove parameters. These parameters still must be varied to achieve prescribed filling and cross-section. This is done by the top-level functions calc_single_groove, calc_single_groove_opened and calc_single_groove_flat. These make use of the minimization algorithm fminsearchbnd by John D'Errico.[12] This is a variant of MATLAB's own minimization algorithm fminsearch, based on the simplex search method by Lagarias.[13] fminsearchbnd allows one to specify prescribed boundaries of the input values that shall not be violated during the iterations, as to ensure that no irrational parameter combinations will be selected by the algorithm.

The calculation scheme is as follows:

First, the groove is created with an assumed initial geometry. Then, the flat-pass data of the equivalent rectangle method is calculated as described in Reference 3. Then the spread calculation is carried out, resulting in an output width of the rolled section b1, as well as the resulting groove filling ratio $f_f = b_1/wof$ and an output cross-section A1. The groove parameters are then varied by the minimization algorithm to bring the residual as close to zero as possible.

Figure 5

Optimization results for single passes from an initial round section of 50 mm and a pass reduction of 20% for different groove filling ratios at non-opened single-radius grooves.

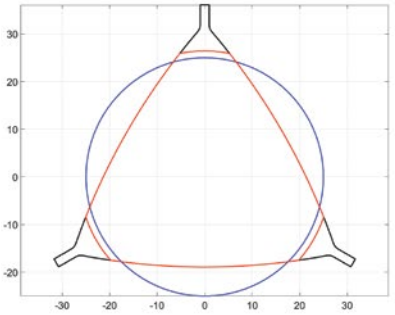

(a)

Filling ratio: 85%
Inner radius: 18.9 mm
Groove radius: 138.5 mm

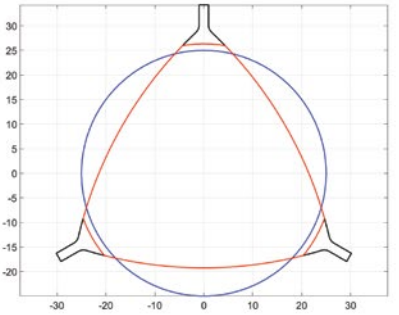

(b)

Filling ratio: 90%
Inner radius: 19.26 mm
Groove radius: 83.16 mm

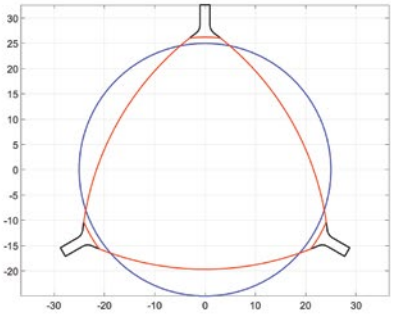

(c)

Filling ratio: 95%
Inner radius: 19.69 mm
Groove radius: 56.84 mm

As a result, the groove data and the numerical contour shape of the groove are obtained, which fulfills the criteria provided by the user.

Exemplified Results for Single Passes on a Circular Entry Section

The first example will look at a pass where an initial round section is deformed in a non-opened single-radius groove.

Fig. 5 shows three pass shapes for an entry diameter of d_0 = 50 mm, a pass reduction of 20% and filling ratios of 85%, 90% and 95% at a nominal roll diameter of d_{nom} = 400 mm.

Generally, when a higher filling ratio is allowed, the groove eccentricity will decrease, resulting in the groove shape shifting from a triangular shape to a more circular shape.

For the opened single-radius groove, it was investigated how the eccentricity values of the grooves change at a fixed filling ratio and pass reduction, when the opening angle is varied. Fig. 6 shows three passes that were calculated to achieve a 95% filling ratio at opening angles between 50° and 70°. The small circles indicate the positions on the roll barrel of the right roll where the tangential opened part of the roll barrel transitions into the main radius part.

Table 2 shows the details of the calculations. Note that in the first calculation for 50°, the anticipated filling ratio and pass reduction values could not be achieved exactly, as the algorithm was bound to not use eccentricity values less than 1.

In looking at practical pass designs of 3-roll rolling mills, it is quite uncommon for these opened grooves to be used at very high eccentricity values. Therefore,

Figure 6

Calculated groove shapes and rolling passes for opened single-radius grooves with different opening angles at a filling ratio of 95% (a: 50°, b: 60°, c: 70°).

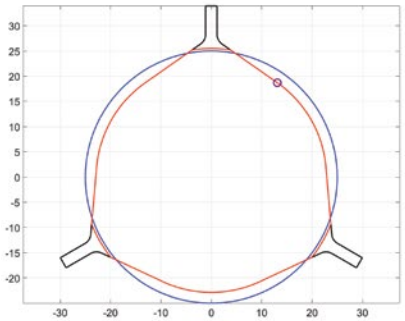

(a)

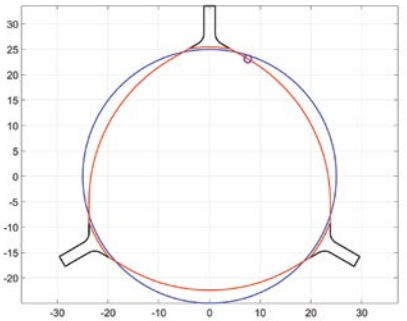

(b)

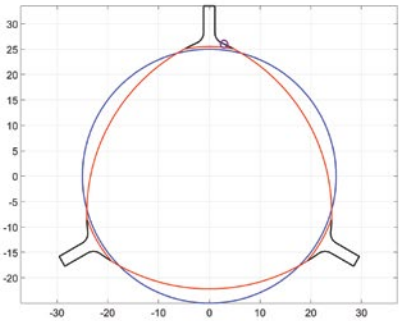

(c)

Table 2

Calculation Results for the Opened Single-Radius Groove Examples Shown in Fig. 6

Opening angle	Inner radius IR	Main radius R1	Eccentricity e = R1/IR	Filling ratio achieved	Cross-sectional reduction	Residual value
50°	22.842 mm	22.842 mm	1.000	94.18%	10.67°	0.011
60°	22.432 mm	32.496 mm	1.449	94.995%	9.999°	0.000
70°	22.173 mm	36.721 mm	1.656	95.00%	10.00°	0.000

Figure 7

Pass design results for a pass reduction of 20%, filling ratios 85% (a), 90% (b) and 95% (c) at the eccentricity 1.0 for opened single-radius grooves.

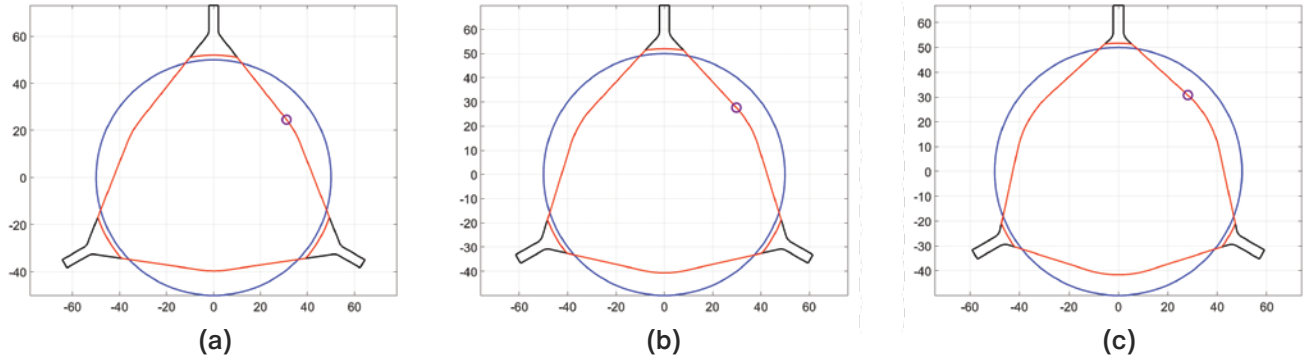

another example is presented in which the eccentricity of the groove is fixed at 1.00 and the necessary opening angle is calculated in order to achieve different filling ratios (see Fig. 7).

Table 3 shows again the parameters of these calculations.

As it can be seen, the opening angle increases with an increasing groove filling ratio. With the optimization algorithm used in the presented software implementation, one can find the opening angles which correspond to a prescribed filling ratio.

Table 3

Calculation Results for the Opened Single-Radius Groove Examples Shown in Fig. 7

Opening angle	Radius IR =R1	Filling ratio achieved	Cross-sectional reduction	Residual value
35.27°	41.666 mm	0.9499	0.1999	0.000
25.52°	40.648 mm	0.9000	0.2000	0.000
16.82°	39.593 mm	0.8500	0.1999	0.000

Calculation of Groove Series

The cases treated so far only include first passes on a circular entry section. On top of that, it is of practical interest to design a complete groove series which transforms a given entry section to a circular output section in a prescribed number of passes. The optimization goal is then to find the groove parameters of each individual rolling stand. This problem can be addressed by repeated application of the present algorithm to each individual groove.

As the algorithm requires prescribed cross-sectional area values, a suitable elongation distribution must first be carried out for the intended pass sequence. The elongation factor of pass i will be called λ_i and can be given in the following way:

$$\lambda_i = \lambda_m \cdot Z^y$$

(Eq. 14)

The factor Z steers the degree of degression, and y is again a function of i:

$$y = \frac{N+1}{2} - i$$

(Eq. 15)

The total elongation is still given by the product of all single-stand elongations, and this approach ensures that all pass elongations still lead to the prescribed total elongation. It will be seen later that the choice of the degression factor Z is crucial to reach the final section size.

Now for the example of an initial circular cross-section with the diameter d_0 = 40 mm, which shall be reduced to a final diameter of d_f = 20 mm in six passes with a nominal roll diameter of d_N = 400 mm. If the design of the elongation distribution is performed according to Eq. 14, one may encounter high reductions in the first pass. As the entry to the first pass is still a round section, the possible reductions are somewhat limited. Therefore, one may want to limit the first pass reduction to, say, 20% or 25%. The remaining deformation is then further distributed to the remaining passes. The second pass can take a higher deformation because a sharp triangular section will exit the first pass.

The pass-by-pass application of the methodology described in the preceding section is now carried out for all passes except the last one, as a well-defined exit section is generally required and therefore the final groove

Figure 8

The final groove with entry and exit sections for different distribution factors Z (a: Z=1.05, b: Z=1.09, c: Z=1.12).

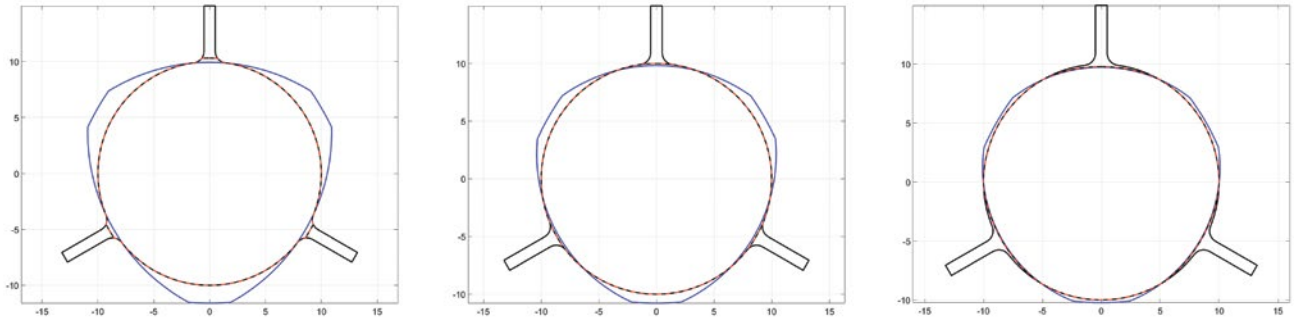

(a) (b) (c)

Table 4

Pass Design Data for the Rolling Case According to Fig. 8b

Pass No.	Inner radius of groove IR	Main radius of groove R1	Eccentricity R1/IR	Calculated filling ratio	Pass reduction
1	15.580	51.159	3.284	0.95	20 %
2	12.217	72.399	5.926	0.95	33 %
3	11.113	27.841	2.505	0.95	27 %
4	10.081	21.098	2.093	0.95	21 %
5	9.820	14.056	1.431	0.95	14 %
6	10.000	10.000	1.000	0.9985	6 %

should be completely prescribed. Therefore, there is no possibility to influence the filling of the last pass other than the size of its entry section. It follows that the degression factor Z must be adjusted to match the anticipated exit section.

Fig. 8 shows three examples for the dependency of the output section on the degression factor, for the rolling task under consideration (40 mm to 20 mm in six passes).

The first case was calculated using a value of Z = 1.05. As it can be seen, the entry section to the last pass is too big because too little deformation is carried out before the last pass — the elongation distribution is not degressive enough. As a result, too much spreading occurs, and the final groove is overfilled. In the second example, a slightly higher factor of Z = 1.09 is used. The groove filling is just right. Also note the changes of the entry section, which is much more triangular in the first example.

If this effect is reversed and too high a degression factor is used, an underfilled section will result (see Fig. 8c), because the entry cross-section to the last pass was already reduced too much and there is not enough spreading to appear in the last pass as to produce the desired output section.

Finally, Table 4 shows the pass design data encountered for case B with the just right groove filling.

From these data, it can be seen that the eccentricities, as well as the pass reductions, show a degressive pattern from pass 2 on. This is the case because pass 1 was restricted to 20% reduction as explained before. Therefore, pass 2 will have the highest reduction and the highest eccentricity relation. The eccentricity of pass 2 with 5.926 corresponds to a nearly triangular groove with a very high main radius.

Fig. 9 now shows the final plot of the calculated groove shapes according to Table 4.

Conclusions

In this article, a software algorithm for roll pass design of round sections in 3-roll rolling mills was presented.

Figure 9

The calculated pass design for 40-mm to 20-mm circular in six passes.

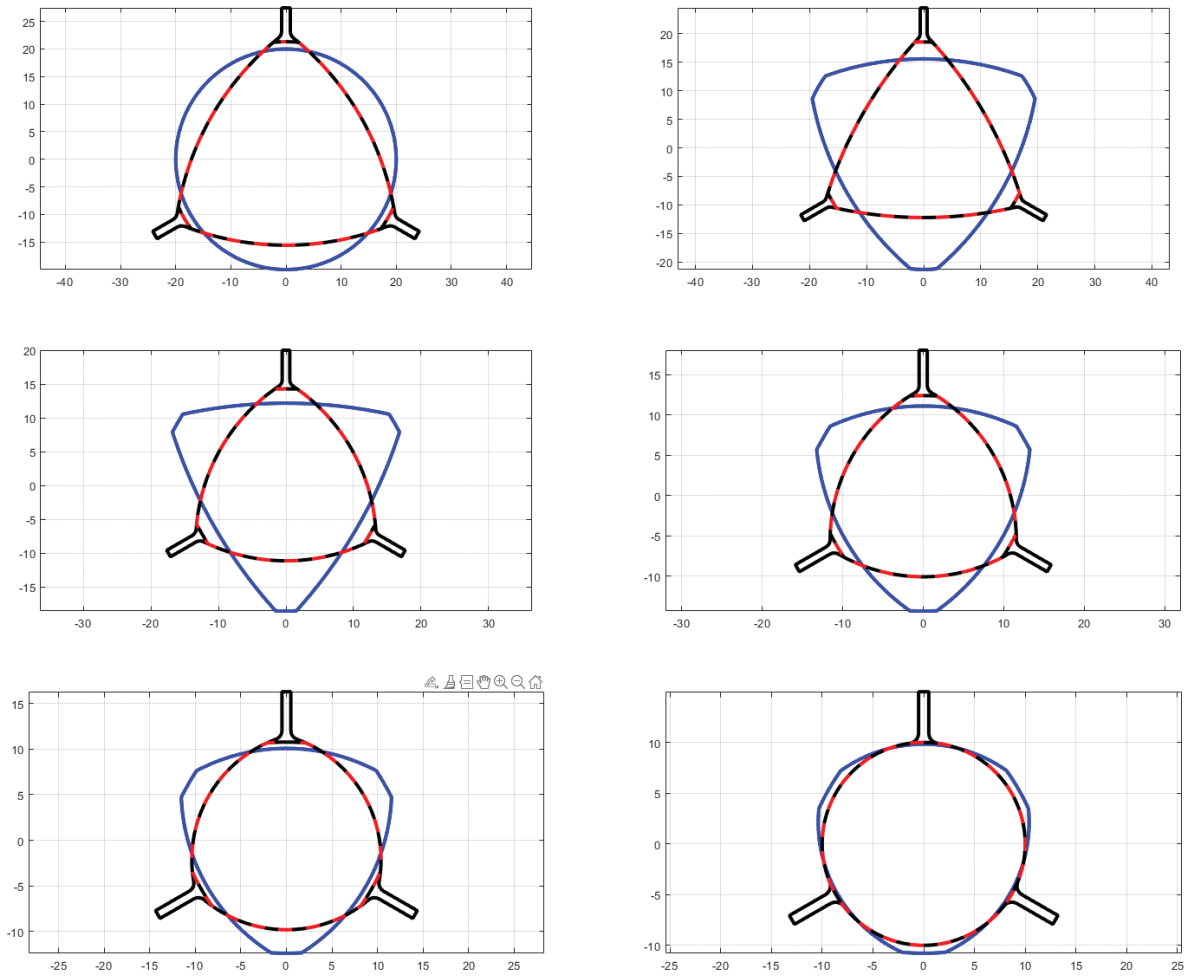

After the fundamentals of the spread calculations were explained, three typical groove geometries (flat, single-radius, opened single-radius) were introduced with their determining geometrical parameters. The very import equations for the width on face are given for the three groove types. After this, an algorithm is described to automatically design a groove geometry with a given entry section and prescribed exit cross-sectional area and filling ratio. For exemplified single passes with an initial circular section, it is shown how the groove shapes evolve as a function of filling and eccentricity relations. Finally, the methodology is applied to generate a pass design for a continuous multistand rolling operation. The algorithm described allows an almost automatic and very fast pass design, where the only manual adjustment needed is that of slight adaption of the prescribed elongation distribution to ensure a final section free from rolling faults.

It can be argued that the method of spread calculation used is a simple transfer from the 2-roll process. However, any other spread calculation model can be readily included in the model by replacing the MATLAB function spread_calculation.

The complete MATLAB source code used in this article is maintained at a GitHub repository at https://github.com/choverhagen/threeroll.

Acknowledgments

This paper is dedicated to the memory of the author's late Ph.D. advisor Prof. Dr. Paul Josef Mauk, who died unexpectedly in January 2018. Ten years ago, he supervised the author's work on the mechanical rolling model for the 3-roll process.

The author wishes to thank the University of Duisburg-Essen for the freedom granted to undertake the research activities which led to the present work.

References

1. C. Overhagen, R. Braun and R. Deike, "Analysis of Elastic Rolling Stand Deformation and Interstand Tension Effects on Section Faults of Hot Rolled Wire Rod and Bars," *tm – Technisches Messen,* 2020, https://doi.org/10.1515/teme-2019-0130.
2. C. Overhagen, "Numerical Assessment of Interstand Tensions in Continuous Hot Rolling Processes of Flat and Long Products," *The International Journal of Advanced Manufacturing Technology,* 2024, https://doi.org/10.1007/s00170-023-11584-x.
3. C. Overhagen and P.J. Mauk, "A New Rolling Model for 3-Roll Rolling Mills," *Key Engineering Materials,* Vols. 622–623, 2014, pp. 879–886, https://doi.org/10.4028/www.scientific.net/KEM.622-623.879.
4. M. Weiner, C. Renzing, M. Stirl, M. Schmidtchen and U. Prahl, "PyRolL – An Extensible OpenSource Framework for Rolling Simulation," *The Journal of Open Source Software,* Vol. 9, No. 93, p. 6200, https://doi.org/10.21105/joss.06200.
5. C. Overhagen, "Models for Rolling Flat and Solid Cross Sections," (in German), Ph.D. eng. thesis, University of Duisburg-Essen, 2018, https://nbn-resolving.org/urn:nbn:de:hbz:464-20181116-114523-7.
6. C. Overhagen and P.J. Mauk, "Flexible Groove Sequences for Hot Rolling a Number of Materials," *AISTech 2012 Conference Proceedings,* 2012.
7. P.J. Mauk and R. Kopp, "Spread Under Hot Rolling – Comparison of Calculation Methods – Exactness – New Results," *Der Kalibreur,* Vol. 37, 1982, pp. 61–68.
8. N. Marini, "New Theory on Lamination," (in Italian) *La Metallurgia Italiana,* 1941, pp. 292–309.
9. M. Horihata and M. Motomura, "Theoretical Analysis of 3-Roll Rolling Process by the Energy Method," *Transactions ISIJ,* Vol. 28, 1988, pp. 434–439.
10. J.H. Min, H.C. Kwon, Y. Lee, J.S. Woo, Y.T. Im, "Analytical Model for Prediction of Deformed Shape in 3-Roll Rolling Process," *Journal of Materials Processing Technology,* Vol. 140, 2003, pp. 471–477, https://doi.org/10.1016/S0924-0136(03)00717-9.
11. C. Overhagen, "Roll Pass Design Methods for Three- and Four-Roll Rolling Mills – Comparison and Analysis," *11th International Rolling Conference, ABM Week,* 2019, São Paulo, SP, Brazil.
12. J. D'Errico, fminsearchbnd, fminsearchcon, https://www.mathworks.com/matlabcentral/fileexchange/8277-fminsearchbnd-fminsearchcon, MATLAB Central File Exchange, retrieved 15 February 2024.
13. J.C. Lagarias, J.A. Reeds, M.H. Wright and P.E. Wright, "Convergence Properties of the Nelder-Mead Simplex Method in Low Dimensions," *SIAM Journal of Optimization,* Vol. 9, No. 1, 1998, pp. 112–147.

AISTech This paper was presented at AISTech 2024 — The Iron & Steel Technology Conference and Exposition, Columbus, Ohio, USA, and published in the AISTech 2024 Conference Proceedings.